

Exploring Bell Nonlocality with Extremal Non-Signaling Boxes

Emmanuel Zambrini Cruzeiro,^{1,2} Junior R. Gonzales-Ureta,³
Raman Choudhary,⁴ Hugo Abreu,⁵ Adán Cabello,^{6,7} and Sébastien Designolle^{5,8}

¹*Quantum Information and Quantum Optics Laboratory, Instituto Superior Técnico, Lisboa, Portugal*

²*Quantum Physics of Information Group, Instituto de Telecomunicações, Lisboa, Portugal*

³*Q*Bird BV, Delftsempark 1, 2628 XJ, Delft, The Netherlands*

⁴*INL – International Iberian Nanotechnology Laboratory, Braga, Portugal*

⁵*Zuse Institute Berlin, Takustraße 7, 14195 Berlin, Germany*

⁶*Departamento de Física Aplicada II, Universidad de Sevilla, E-41012 Sevilla, Spain*

⁷*Instituto Carlos I de Física Teórica y Computacional, Universidad de Sevilla, E-41012 Sevilla, Spain*

⁸*Inria, ENS de Lyon, UCBL, LIP, 69342, Lyon Cedex 07, France*

(Dated: January 15, 2026)

Extremal non-signaling (ENS) boxes are correlations that correspond to vertices of the non-signaling polytope of a Bell scenario. Neither quantum theory nor any theory for ideal measurements allows for ENS boxes. That is, according to quantum theory, ENS boxes are nonphysical. Still, ENS boxes are crucial for addressing a number of problems in Bell nonlocality. Here, we obtain ENS boxes in arbitrary bipartite Bell scenarios and present the complete list of ENS boxes for several unexplored scenarios. Equipped with the boxes, we revisit several foundational questions. We find that already two copies of *any* ENS box violate the exclusivity (or local orthogonality) and Specker’s principles. We provide the minimal decomposition of the magic square correlation—the simplest known perfect correlation in nature—in terms of ENS boxes. We identify the minimal scenario in which a *dit* of communication (with $d \leq 5$) is insufficient to simulate ENS boxes. Our results show that the ENS boxes approach leads to new results and opens new avenues for research.

Introduction.— Extremal non-signaling (ENS) boxes are vertices of the non-signaling (NS) polytope denoted \mathcal{NS} [1]. Some of these are vertices of the local polytope, while others are nonlocal. Neither quantum theory [2] nor any theory for ideal measurements [3] permit the existence of nonlocal ENS boxes. However, these boxes are of fundamental interest to physics because their convex combinations that lie outside the quantum set represent correlations which could be present in some future post-quantum theory. Naturally, knowing the complete set of ENS boxes of a given Bell scenario is necessary to address a large number of problems.

A precise understanding of \mathcal{NS} is central to the study of quantum correlations. Several operational principles have been proposed to explain why quantum correlations are strictly weaker than NS correlations. As such, nonlocal ENS boxes can be used to bound the quantum set from above. It is known that Popescu-Rohrlich (PR) boxes, the only class of nonlocal ENS boxes in the simplest Bell scenario, collapse communication complexity [4], violate information causality [5], macroscopic locality [6], the exclusivity principle [7], and local orthogonality [8]. Nonlocal ENS boxes can shed light on the advantages and limitations of such principles.

One way of characterizing quantum correlations is to compare different resources, i.e., how they can be converted into one another. In Bell nonlocality, one considers correlations stemming from local resources, quantum states and measurements, ENS boxes, and classical communication (signaling). Quantum communication complexity refers to the simulation of quantum correlations using classical communication [9]. Nonlocal ENS boxes can also be simulated using classical or quantum resources. Conversely, one can simulate quantum (or any of the other) correlations using NS resources. For example, one can simulate nonlocality arising from (partially) entangled two-qudit states [10] using ENS boxes. ENS boxes

can be used to study the classical and quantum [11] simulation costs of ENS boxes scaling with the scenario (min. average communication cost), and simulation of quantum behaviors using ENS boxes [9]. Regarding classical communication complexity, it is known that one PR box can be simulated with one bit of communication [12]. This naturally begs the question: what is the smallest scenario with a nonlocal ENS box which cannot be simulated by a bit of classical communication? How about a *dit*? Here, we answer the general question up to $d \leq 5$. One useful direct implication of these results are upper bounds on the amount of PR boxes required to simulate a given nonlocal ENS box.

In this work, we directly construct a large number of ENS boxes in arbitrary bipartite scenarios by combining the ideas of Jones *et al.* [13] and Barrett *et al.* [14] and checking which of our guesses are indeed extremal.

Using this prior information on the ENS boxes, we can solve the vertex enumeration problem for several small scenarios that were intractable before. We then present several contributions to bipartite Bell nonlocality by constructing ENS boxes and using them for three different problems. Firstly, using vertex enumeration with prior knowledge of vertices, we find the complete lists of ENS boxes for various scenarios such as $(2,3,3,2)$, $(3,3,3,2)$, $(2,3,3,3)$, $(3,3,3,3)$, $(5,4,2,2)$, and more. We provide a database with the lists of ENS boxes along with the article. Secondly, we use the boxes to show that for all the corresponding scenarios, two copies of any ENS box are sufficient to violate local orthogonality. This is in line with what is already known for previously known bipartite ENS boxes. Thirdly, we provide examples of nonlocal ENS boxes which cannot be reproduced by one *dit* of classical communication, up to $d \leq 5$. Finally, we obtain decompositions of the magic square correlations in terms of ENS boxes, the minimum of which includes two boxes.

State of the art.— In a bipartite Bell scenario, Alice (Bob) has X (Y) input settings and A (B) outcomes. We denote such a scenario (X, Y, A, B) . In the tripartite case, we add input and output cardinalities Z and C , respectively, for the third party (Charlie). The notation becomes (X, Y, Z, A, B, C) . Complete lists of ENS boxes are available for scenarios $(d, d, 2, 2)$ [13], $(2, 2, d, d)$ [14], and $(2, 2, 2, 2, 2, 2)$ [15], for any integer $d \geq 2$. Some nonlocal ENS boxes are known in $(d, 2, d, d)$ [16], and are constructed using the same ideas found in [14]. Finding nonlocal ENS boxes beyond these cases is a long-standing open problem.

There are multiple choices for specialized facet/vertex enumeration software out there, but few of them have as many useful functionalities as PANDA [17]. Specifically for the purpose of our work here, two of them are very relevant: (i) the possibility to speed up the facet/vertex enumeration solving by providing PANDA with known facets/vertices, (ii) PANDA will directly provide the classes of facets/vertices so long as we provide it with the generators of the symmetry group. Thanks to (i) and (ii), we systematically characterize \mathcal{NS} in this work, providing in some cases the complete list of classes of ENS boxes of a given Bell scenario. To feed PANDA with as much data about known ENS boxes as possible, we guess (in an educated way) nonlocal ENS boxes. Our method combines ideas of Masanes *et al.* [13] and Barrett *et al.* [14] to generate ENS boxes in bipartite Bell scenario where $A = B$. We show below that some of these boxes are extremal, so that we call them *potential* ENS boxes.

Formally, for $A = B$, they are defined as follows:

$$\begin{pmatrix} S & S & \dots & S & L & \dots & L \\ S & T_{2,2} & \dots & T_{2,Y-h} & L & \dots & L \\ \vdots & \vdots & \ddots & \vdots & \vdots & \ddots & \vdots \\ S & T_{X-g,2} & \dots & T_{X-g,Y-h} & L & \dots & L \\ K & K & \dots & K & M & \dots & M \\ \vdots & \vdots & \ddots & \vdots & \vdots & \ddots & \vdots \\ K & K & \dots & K & M & \dots & M \end{pmatrix}, \quad (1)$$

where $g \in \{2, \dots, X\}$ and $h \in \{2, \dots, Y\}$. The $A \times A$ matrix blocks are defined as follows: S (resp. K and L) is filled with $1/A$ on the diagonal (resp. first line and column), M has a one in its first entry, and $A \cdot T_{i,j}$ is any circulant matrix. For $A = 2$, this definition matches precisely the family defined in [13], so that all these boxes are extremal. For $A > 2$, PANDA can be used to check extremality: for all the scenarios we have studied (see Fig. 2), restricting to $A \cdot T_{i,j}$ being of order coprime with A yields ENS boxes. This criterion typically excludes $\sigma_x \otimes \mathbb{1}$ for $A = 4$.

Complete lists of ENS boxes.— Using PANDA and prior information of known vertices, we analyzed and classified all the ENS boxes in a variety of scenarios. The scenarios are shown in Fig. 2 and Table I. We further classify the ENS boxes into full-output and partial-output vertices, in the scenarios $(2, 3, 3, 2)$, $(3, 3, 3, 2)$, and $(2, 3, 3, 3)$. This analysis can be found in the Supplemental Material. In some scenarios, we conjecture the list is complete. For example, in $(3, 3, 3, 3)$,

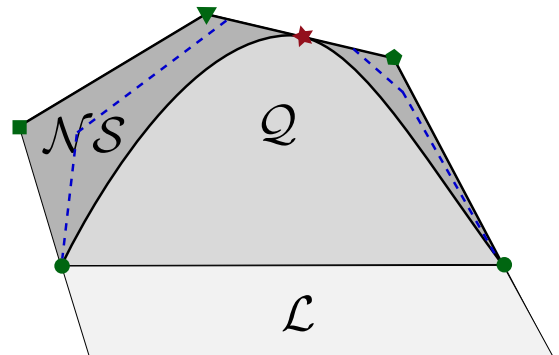


FIG. 1. Geometric depiction of our main findings described with respect to different correlation sets: local (\mathcal{L} , inner set, white), quantum (\mathcal{Q} , light gray), and non-signaling (\mathcal{NS} , dark gray). Note that $\text{LO}^{(1)} = \mathcal{NS}$, whereas $\text{LO}^{(2)}$ is drawn with blue dashed lines. While local vertices are indicated by green disks, nonlocal non-signaling vertices are distinguished by three different green markers (square, pentagon, and triangle, illustrating the different amounts of classical communication needed to simulate these boxes. The red star represents magic square correlations, which we show can be decomposed into a convex combination of two ENS boxes.

we find 8147 classes of boxes, which we conjecture to be the complete list of ENS boxes for that scenario. All the results are provided in a database [18].

Violations of Local Orthogonality.— Bounding the quantum set of nonlocal correlations from information-theoretic and physical principles is an open problem [7, 19]. One principle which is useful for this task is local orthogonality, which is the name sometimes given in the literature to the exclusivity principle [20] in Bell scenarios. In some frameworks, the exclusivity principle is not a principle but a theorem. For example, it has to be satisfied for theories of minimally disturbing measurements [21, 22]. In [23, 24], the authors explored all nonlocal ENS boxes of bipartite scenarios $(2, 2, 2, 2)$, $(m, m, 2, 2)$, $(2, 2, d, d)$, and the tripartite scenario $(2, 2, 2, 2, 2, 2)$ to obtain violations of the Local orthogonality (LO) principle. Their main result can be summarized as follows: each of the bipartite ENS boxes that they considered necessarily requires two statistically independent copies of the box to violate the LO principle, while only one copy of the tripartite box violates an LO inequality. The former is expressed as the violation of the LO^2 inequality while the latter is defined as the violation of LO^1 inequality. A natural question is: can we find examples of ENS correlations which satisfy every LO^2 inequality? It is already shown in [23, 25] that for any single copy of a bipartite scenario the set of correlations satisfying LO^1 is the same as the set of correlations satisfying the NS principle. Therefore, for each of the ENS boxes found in this work, we look for the violation of some LO^2 inequality.

It is also well established that the problem of finding violation of LO^k inequalities can be mapped to finding a sufficiently large clique (complete graph) inside the joint exclusivity graph of k copies of the scenario, formed by taking the OR product of all k copies of the correlation under consideration. Note that it is the clique size as well as node weights that determine the violation. For extremal boxes, like the famous PR

box, where all possible events occur with the same probability, i.e., the corresponding graph has uniform node weights, the violation only depends on the size of the clique but more generally it is the size as well as the node weights of the clique that determine violations of corresponding LO inequalities.

For example, consider the ENS box given in Eq. (A1). Focusing on LO² means considering two statistically independent copies of this box. This means that if e_i^1 and e_j^2 are possible events from two different copies of the extremal box, and the joint event is denoted by (e_i^1, e_j^2) , then $P(e_i^1, e_j^2) = P(e_i^1)P(e_j^2)$.

For the extremal box in Eq. (A1), there are only three possible values of the joint probability of any event (e_i^1, e_j^2) : $\frac{1}{4}$, $\frac{1}{16}$, and $\frac{1}{8}$. $\frac{1}{4}$ when $P(e_i^1) = P(e_j^2) = \frac{1}{2}$, $\frac{1}{16}$ when $P(e_i^1) = P(e_j^2) = \frac{1}{4}$, and $\frac{1}{8}$ when either one of $P(e_i^1)$ or $P(e_j^2)$ is $\frac{1}{4}$ while the other one is $\frac{1}{2}$. This means that for any clique (composed of two independent joint events coming from two copies of the extremal box) that has x nodes assigning probability $\frac{1}{4}$, y nodes assigning probability $\frac{1}{16}$, and z nodes assigning probability $\frac{1}{8}$, the condition of violation of the LO² inequality corresponding to this clique (of size $x + y + z$) is:

$$\frac{x}{4} + \frac{y}{16} + \frac{z}{8} > 1, \quad (2)$$

or equivalently, $4x + y + 2z > 16$. In general, if k is the size of the clique, i.e., $x + y + z = k$, then any solution to this equation must satisfy the following to violate the LO² inequality, $3x + z > 16 - k$. It can be algebraically argued that no solution to the equation $x + y + z \leq 4$ violates inequality (2). Therefore, the smallest clique potentially violating the LO² inequality has size $k \geq 5$. It can be further logically argued that no $k = 5$ sized clique would provide violation as well. Informed by this, we ran a code that tested if any clique of size more than 5 exists to violate the LO² inequality, to which we found a K_9 providing the violation. The set of these 9 locally orthogonal events being: $\{1120|0011, 1001|1212, 2010|0010, 0121|1021, 2101|0220, 2020|0010, 2111|0220, 0101|0221, 0120|0011\}$.

The same analysis is provided for other examples of boxes in Section D. For the boxes considered with binary outcomes, the violated inequality LO² always corresponds to a K_5 . The same is true for binary outcome bipartite ENS boxes considered in [24]. Furthermore, for all classes of ENS boxes with more than binary outcomes, we also find a violation of some LO² inequality. We conjecture that in bipartite Bell scenarios, two copies of any ENS box always violate some LO² inequality. Note that this is not true in general: the tripartite ENS boxes for (2,2,2,2,2,2) mentioned previously does violate an LO¹ inequality, and consequently an LO² inequality as well, whereas extremal boxes for certain Kochen-Specker scenarios even do not violate inequalities corresponding to LO³ as shown in [26].

Communication complexity of ENS boxes.— A fundamental step for understanding why some correlations are impossible is quantifying their simulation cost. Here, we present new results on the amount of classical communication required to simulate ENS boxes. Using the Frank-Wolfe technique

in [27, 28] adapted for local hidden variable models supplemented with classical communication, we systematically look for violations of the one *dit* polytope. In Table II of the Supplemental Material, we provide the number of boxes which violate each case, along with the minimum visibility for that scenario. This allows us to provide minimal examples of ENS boxes that cannot be simulated by a *dit* of communication, for $d \leq 5$. The highest communication complexity being achieved in the scenario (6, 4, 2, 2). Along with these behaviors, we provide facets separating them from the polytope of local correlations with supplementary classical *dit* communication.

We find that the (3,3,3,3) ENS box first presented in [13] can be simulated with one bit of communication. In contrast, 8160 out of the 8747 classes of boxes cannot be reproduced with one bit, i.e., require a trit.

It turns out that the scenario $(m, m, 2, 2)$, already solved in [13], allows to generalize the pattern that emerges from Table IIa. In this scenario, consider the following extremal NS probability distribution (in the matrix-matrix notation from [13])

$$p = \begin{pmatrix} C & C & \cdots & C \\ C & A & \cdots & C \\ \vdots & \vdots & \ddots & \vdots \\ C & C & \cdots & A \end{pmatrix}, \quad (3)$$

where $C = \frac{1}{2} \begin{pmatrix} 1 & 0 \\ 0 & 1 \end{pmatrix}$ and $A = \frac{1}{2} \begin{pmatrix} 0 & 1 \\ 1 & 0 \end{pmatrix}$. Define $F = 4p - 1$; the value attained by p for this inequality is m^2 , while we prove in Section E that the bounds with communication $d \leq m$ are $L_d = m^2 - 2(m - d)$. This shows that p is not in LHV+($m - 1$)it. Note that the inequality F generalizes CHSH in a way that strongly favors NS strategies at the expense of quantum ones. The quantum value is indeed $2\sqrt{2}$ for $m = 2$, 6 for $m = 3$ (still nonlocal), but it then coincides with the local bound for $m \geq 4$.

The minimal decomposition of the Magic square correlations.— The magic square correlations win the magic square game with probability one [19]. For our purpose it is more handy to use the Bell inequality formulation of the magic square game [19], details in the Supplemental Material. In this framework the magic square correlations belong to the (3,3,4,4) scenario, and they are given by

$$\vec{p}_{MS} = \frac{1}{8} \times \begin{pmatrix} 1 & 1 & & & & & & \\ 1 & 1 & & & & & & \\ & & 1 & 1 & 1 & 1 & & \\ & & 1 & 1 & & & 1 & 1 \\ \hline 1 & 1 & 1 & 1 & & & 1 & 1 \\ 1 & 1 & & & 1 & 1 & 1 & 1 \\ 1 & 1 & 1 & 1 & 1 & 1 & 1 & 1 \\ 1 & 1 & & & 1 & 1 & 1 & 1 \\ \hline 1 & 1 & 1 & 1 & 1 & 1 & 1 & 1 \\ 1 & 1 & & & 1 & 1 & 1 & 1 \\ 1 & 1 & 1 & 1 & 1 & 1 & 1 & 1 \\ 1 & 1 & & & 1 & 1 & 1 & 1 \end{pmatrix}. \quad (4)$$

We begin by finding the minimum decomposition of \vec{p}_{MS} in terms of ENS boxes without relying on vertex enumeration. Let us consider that the magic square correlations can be decomposed as the mid point of two extremal NS boxes, that is, there are two vectors $\vec{p}_{MS} \pm \vec{v}$ that belong to \mathcal{NS} with $\vec{v} \neq 0$.

Using the positivity, normalization, and NS conditions over $\vec{p}_{MS} \pm \vec{v}$ we can derive a set of conditions for the components of \vec{v} . These conditions do not fix completely \vec{v} but we can choose values for it aiming to satisfy with equality the maximum number of positivity constraints for $\vec{p}_{MS} \pm \vec{v}$. With this choice of \vec{v} we can obtain the two correlations

$$\vec{p}_1 = \frac{1}{4} \times \begin{pmatrix} 1 & 1 & 1 & 1 \\ 1 & 1 & 1 & 1 \\ 1 & 1 & 1 & 1 \\ 1 & 1 & 1 & 1 \\ \hline 1 & 1 & 1 & 1 \\ 1 & 1 & 1 & 1 \\ 1 & 1 & 1 & 1 \\ 1 & 1 & 1 & 1 \\ \hline 1 & 1 & 1 & 1 \\ 1 & 1 & 1 & 1 \\ 1 & 1 & 1 & 1 \\ 1 & 1 & 1 & 1 \end{pmatrix}, \quad \vec{p}_2 = \frac{1}{4} \times \begin{pmatrix} 1 & 1 & 1 & 1 \\ 1 & 1 & 1 & 1 \\ 1 & 1 & 1 & 1 \\ 1 & 1 & 1 & 1 \\ \hline 1 & 1 & 1 & 1 \\ 1 & 1 & 1 & 1 \\ 1 & 1 & 1 & 1 \\ 1 & 1 & 1 & 1 \\ \hline 1 & 1 & 1 & 1 \\ 1 & 1 & 1 & 1 \\ 1 & 1 & 1 & 1 \\ 1 & 1 & 1 & 1 \end{pmatrix} \quad (5)$$

Moreover, it is possible to show that \vec{p}_1 and \vec{p}_2 cannot be written as convex combination of other NS correlations, or equivalently that $(\vec{p}_i \pm \vec{v}) \in \mathcal{NS}$ is true only when $\vec{v} = 0$.

Note that these are ENS boxes, so we could also have obtained the decomposition directly thanks to the previous results.

It is also interesting to decompose the magic square correlations in terms of PR boxes, similar to what was done in [15]. One possibility is to change the choice of \vec{v} to aim at partial-input ENS boxes. In this case the method does not yield immediately the decomposition, because it is not possible to decompose the magic square correlations as the mid point of two partial-input ENS boxes. However, after three iterations of the method we arrive at a decomposition with 8 ENS vertices

$$\vec{p}_{MS} = \frac{1}{8} \sum_{i=1}^8 \vec{q}_i, \text{ with } \vec{q}_1 = \frac{1}{2} \times \begin{pmatrix} 2 & 1 & 1 & 1 & 1 & 1 \\ 1 & 1 & 1 & 1 & 1 & 1 \\ 1 & 1 & 1 & 1 & 1 & 1 \\ 1 & 1 & 1 & 1 & 1 & 1 \\ \hline 1 & 1 & 1 & 1 & 1 & 1 \\ 1 & 1 & 1 & 1 & 1 & 1 \\ 1 & 1 & 1 & 1 & 1 & 1 \\ 1 & 1 & 1 & 1 & 1 & 1 \end{pmatrix}, \quad (6)$$

and the remaining \vec{q}_i have a similar form. Note that each block consists of a 4×4 matrix. In this decomposition we can see the structure for the inputs $(x, y) = (2, 2), (2, 3), (3, 2), (3, 3)$ is a PR box for two outcomes, while the remaining entries have the structure of the boxes found in Masanes *et al.* [29].

Discussion.— PR boxes have been a crucial tool for understanding quantum correlations and framing more general theories. However, PR are boxes are just *one* example of extremal ENS boxes. Each Bell scenario has their own set. Therefore,

the same reasons why PR boxes are of interest lead to the fundamental question of what the corresponding tools in more general scenarios are, why these tools do not exist, what their simulation cost is, and how existing correlations can be understood in terms of ENS boxes. In this Letter, we have introduced methods and results in all these areas that we expect open a fruitful path for research and provide a new perspective on quantum correlations.

We introduce a multitude of ENS boxes within Bell scenarios, focusing on the bipartite case where a large number of problems can already be addressed. We find that two copies of any ENS box presented here violate the exclusivity principle and local orthogonality, and conjecture this to be a property of any bipartite Bell scenario. Furthermore, we identify the simplest ENS boxes — up to dimension $d \geq 5$ — that cannot be simulated by one dit of classical communication. Finally, we provide a minimal decomposition of the magic square correlations in terms of ENS boxes, with additional convex ENS box decompositions of these correlations presented in the Supplemental Material.

The results presented here offer several promising directions to address other fascinating open problems. First, they can be used to generate new Bell inequalities using the techniques in [30–32] and to find minimal ENS box decompositions of fully nonlocal, post-quantum correlations [33]. Second, we have only explored one principle — the exclusivity principle/local orthogonality — for bounding the quantum set from above using NS correlations. Several other principles offer rich avenues for further investigation. Finally, ENS boxes also have important applications in quantum communication, since they can be used to generate randomness from arbitrarily weak seeds, which requires Hardy-type behavior or pseudotelepathy [34], and are valuable in QKD security proofs under the worst-case assumption of a no-signaling adversary [13].

ACKNOWLEDGMENTS

E.Z.C. acknowledges funding by FCT/MCTES - Fundação para a Ciência e a Tecnologia (Portugal) - through national funds and when applicable co-funding by EU funds under the project UIDB/50008/2020. A.C. was supported by EU funded project FoQaCiA. H.A. and S.D. were supported through the Research Campus Modal funded by the German Federal Ministry of Education and Research (fund numbers 05M14ZAM, 05M20ZBM). S.D. was partly funded by the QuantERA II Programme that has received funding from the European Union's Horizon 2020 research and innovation programme under Grant Agreement No 101017733 (VERIqTAS).

[1] I. Pitowsky, *Quantum Probability-Quantum Logic*, Lecture Notes in Physics, Vol. 321 (Springer-Verlag, Berlin, 1989).
[2] R. Ramanathan, J. Tuziemski, M. Horodecki, and P. Horodecki, *Phys. Rev. Lett.* **117**, 050401 (2016).
[3] Y. Liu, H. Y. Chung, E. Z. Cruzeiro, J. R. Gonzales-Ureta, R. Ramanathan, and A. Cabello, *Phys. Rev. Res.* **6**, L042035 (2024).
[4] W. van Dam, *Nonlocality & Communication Complexity*, Ph.D. thesis, University of Oxford (1999), chapter 9.
[5] M. Pawłowski, T. Paterek, D. Kaszlikowski, V. Scarani, A. Win-

ter, and M. Żukowski, *Nature* **461**, 1101 (2009).

[6] M. Navascués and H. Wunderlich, *Proc. R. Soc. A* **466**, 881 (2010).

[7] A. Cabello, *Phys. Rev. Lett.* **110**, 060402 (2013).

[8] T. Fritz, A. B. Sainz, R. Augusiak, J. B. Brask, R. Chaves, A. Leverrier, and A. Acín, *Nat. Commun.* **4**, 1 (2013).

[9] H. Buhrman, R. Cleve, S. Massar, and R. de Wolf, *Rev. Mod. Phys.* **82**, 665 (2010).

[10] N. Brunner, N. Gisin, S. Popescu, and V. Scarani, *Phys. Rev. A* **78**, 052111 (2008).

[11] R. Ramanathan, M. Banacki, R. Ravell Rodríguez, and P. Horodecki, *npj Quantum Information* **8**, 119 (2022).

[12] W. Van Dam, *Natural Computing* **12**, 9 (2013).

[13] L. Masanes, R. Renner, M. Christandl, A. Winter, and J. Barrett, *IEEE Trans. Inf. Theory* **60**, 4973 (2014).

[14] J. Barrett, N. Linden, S. Massar, S. Pironio, S. Popescu, and D. Roberts, *Phys. Rev. A* **71**, 022101 (2005).

[15] S. Pironio, J.-D. Bancal, and V. Scarani, *J. Phys. A: Math. Theor.* **44**, 065303 (2011).

[16] D. Cavalcanti, A. Salles, and V. Scarani, *Nat. Commun.* **1**, 136 (2010).

[17] S. Lörlwald and G. Reinelt, *EURO J. Comput. Optim.* **3**, 297 (2015).

[18] <https://github.com/sebastiendesignolle/ENS-boxes>.

[19] A. Cabello, *Phys. Rev. Lett.* **87**, 010403 (2001).

[20] A. Cabello, *Phys. Rev. Lett.* **110**, 060402 (2013).

[21] A. Cabello, *Phys. Rev. A* **100**, 032120 (2019).

[22] G. Chiribella, A. Cabello, M. Kleinmann, and M. P. Müller, *Physical Review Research* **2**, 042001 (2020).

[23] A. B. Sainz, T. Fritz, R. Augusiak, J. B. Brask, R. Chaves, A. Leverrier, and A. Acín, *Phys. Rev. A* **89**, 032117 (2014).

[24] T. Fritz, A. B. Sainz, R. Augusiak, J. B. Brask, R. Chaves, A. Leverrier, and A. Acín, *Nat. Commun.* **4**, 2263 (2013).

[25] A. Cabello, S. Severini, and A. Winter, [arXiv:1010.2163](https://arxiv.org/abs/1010.2163) (2010).

[26] R. Choudhary and R. S. Barbosa, [arXiv:2411.09773](https://arxiv.org/abs/2411.09773) (2024).

[27] S. Designolle, G. Iommazzo, M. Besançon, S. Knebel, P. Gelß, and S. Pokutta, *Phys. Rev. Res.* **5**, 043059 (2023).

[28] G. Braun, A. Carderera, C. W. Combettes, H. Hassani, A. Karbasi, A. Mokhtari, and S. Pokutta, [arXiv:2211.14103](https://arxiv.org/abs/2211.14103) (2022).

[29] N. S. Jones and L. Masanes, *Phys. Rev. A* **72**, 052312 (2005).

[30] N. Brunner, V. Scarani, and N. Gisin, *J. Math. Phys.* **47** (2006).

[31] E. Wolfe and S. F. Yelin, *Phys. Rev. A* **86**, 012123 (2012).

[32] T. Cope and R. Colbeck, *Phys. Rev. A* **100**, 022114 (2019).

[33] R. Ramanathan, *Phys. Rev. Res.* **3**, 033100 (2021).

[34] Y. Liu, H. Y. Chung, and R. Ramanathan, *Quantum* **8**, 1489 (2024).

Appendix A: ENS boxes in small Bell scenarios

We analyzed and classified all the ENS boxes, full-output and partial-output, in the scenarios $(2, 3, 3, 2)$, $(3, 3, 3, 2)$, and $(2, 3, 3, 3)$. Notice, we are following the terminology introduced in [14]. Thus, we refer to correlations with all marginals, $p(a|x)$ and $p(b|y)$, greater than zero as “full-output” correlations. While, when at least one marginal is equal to zero, these correlations are called “partial-output”.

1. Scenario $(2, 3, 3, 2)$

In this case there are four ENS boxes. One of them is local, that up to relabelings generates all the vertices of the local polytope for this scenario. The remaining three vertices are nonlocal. Among these three classes none of them is full-output.

2. Scenario $(3, 3, 3, 2)$

In this case there are 16 classes of nonlocal ENS boxes, from these only two are full-output $V_{(3,3,3,2)}^1$ and $V_{(3,3,3,2)}^2$.

$$V_{(3,3,3,2)}^1 = \frac{1}{4} \times \left(\begin{array}{c|cc|c} 1 & 1 & 1 & 1 \\ 1 & 1 & 1 & 1 \\ \hline 2 & 2 & 2 & 2 \\ \hline 2 & 2 & 2 & 2 \\ 1 & 1 & 1 & 1 \\ 1 & 1 & 1 & 1 \\ \hline 1 & 1 & 1 & 1 \\ 1 & 1 & 1 & 1 \\ 2 & 2 & 2 & 2 \end{array} \right), \quad (\text{A1})$$

$$V_{(3,3,3,2)}^2 = \frac{1}{3} \times \left(\begin{array}{c|cc|c} 1 & 1 & 1 & 1 \\ 1 & 1 & 1 & 1 \\ \hline 1 & 1 & 1 & 1 \\ \hline 1 & 1 & 1 & 1 \\ 1 & 1 & 1 & 1 \\ 1 & 1 & 1 & 1 \\ \hline 1 & 1 & 1 & 1 \\ 1 & 1 & 1 & 1 \\ 1 & 1 & 1 & 1 \end{array} \right). \quad (\text{A2})$$

3. Scenario $(2, 3, 3, 3)$

In this scenario there are 22 classes of nonlocal NS vertices, from these, six are full output vertices. Three examples are shown next. These have 34, 35, and 36 zeros.

$$V_{(2,3,3,3)}^{34} = \frac{1}{4} \times \left(\begin{array}{c|cc|c} 2 & 2 & 2 & 2 \\ 1 & 1 & 1 & 1 \\ \hline 1 & 1 & 1 & 1 \\ \hline 1 & 1 & 1 & 1 \\ 1 & 1 & 1 & 1 \\ 1 & 1 & 1 & 1 \\ \hline 1 & 1 & 1 & 2 \end{array} \right), \quad (\text{A3})$$

$$V_{(2,3,3,3)}^{35} = \frac{1}{4} \times \left(\begin{array}{c|c|c|c} 1 & 1 & 1 & 1 \\ \hline 1 & 1 & 1 & 1 \\ \hline 2 & 2 & 1 & 1 \\ \hline 1 & 1 & 1 & 1 \\ \hline 1 & 2 & & 2 \end{array} \right), \quad (\text{A4})$$

$$V_{(2,3,3,3)}^{36} = \frac{1}{3} \times \left(\begin{array}{c|c|c|c} 1 & 1 & 1 & 1 \\ \hline 1 & 1 & 1 & 1 \\ \hline 1 & 1 & 1 & 1 \\ \hline 1 & 1 & 1 & 1 \\ \hline 1 & 1 & & 1 \end{array} \right). \quad (\text{A5})$$

Appendix B: A family of full-output vertices in (X, Y, d, d)

In Fig. 2 and Table I, we summarize the scenarios for which we have obtained complete or partial lists of ENS boxes.

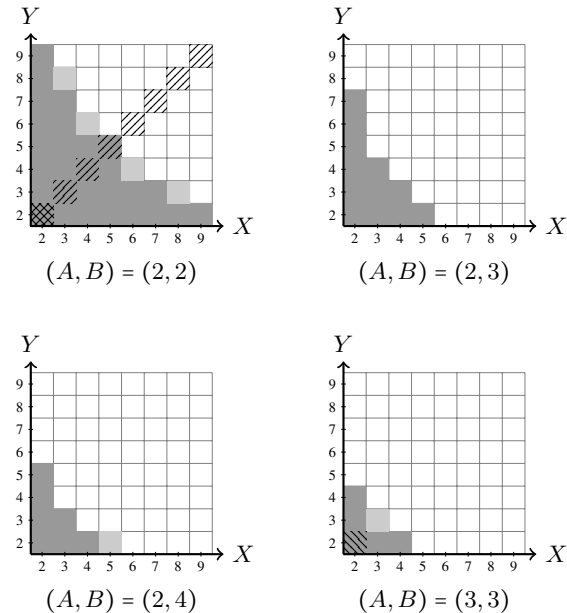


FIG. 2. Illustration showing the bipartite Bell scenarios for which the complete list of ENS boxes is now known. Dark gray cells indicate scenarios solved in this work, while light gray ones correspond to scenarios for which we only conjecture our list of extreme points to be complete. The scenarios $(2, 2, d, d)$ and $(d, d, 2, 2)$ were respectively solved in [13, 14] and are shown with hatch patterns.

It is clear that a wider variety of boxes appear when the number of inputs and outputs is greater than two, as it is exemplified by the scenario $(2,3,3,3)$ in the previous section. Thus,

(X, Y, A, B)	#L1	Ref.
$(2, 2, 3, 4)$	2	This work
$(2, 2, 4, 4)$	3	[14]
$(2, 2, 5, 5)$	4	[14]
$(2, 3, 3, 4)$	28	This work
$(2, 3, 4, 3)$	104	This work

TABLE I. Number of classes of nonlocal ENS boxes. For each scenario, we provide a complete list of classes. The total number of classes is the number of nonlocal ones (column #L1) plus one.

a complete characterization for arbitrary scenarios is an increasingly complex task. However, it is possible to still make progress in the problem by providing partial characterizations in scenarios with particular properties. For instance, we derive a family of full-output ENS boxes in scenarios where the number of zeros in the table of correlations Z is equal to $\dim(\mathcal{NS})$, the dimension of the corresponding NS polytope.

In any scenario with $X \geq 2$ and $Y \geq 2$ the inequality $Z \leq \dim(\mathcal{NS})$ holds. Therefore there are NS vertices with the maximum number of zeros. In fact we can follow the same argument as in [14] and find that there is a family of vertices of the following form

$$p(a, b|x, y) = \left(\begin{array}{c|c|c|c|c} D & D & D & \dots & D \\ \hline D & P^k & P & \dots & P \\ \hline D & P & P & \dots & P \\ \hline \vdots & \vdots & \vdots & & \vdots \\ \hline D & P & P & \dots & P \end{array} \right). \quad (\text{B1})$$

Where D is a diagonal matrix, P^k is a permutation of order k , and P is a permutation of any order. In addition every probability in the table is equal to $1/d$.

One example of this type of vertices is, after relabelings, $V_{(2,3,3,3)}^{36}$. The construction in Eq. (B1) is a natural generalization of the boxes derived in [14] and [29].

Appendix C: The magic square correlations

The result in [2] implies that the correlations that win the magic square game are not an extremal point in \mathcal{NS} . Thus, it is possible to write them as a convex combination of ENS boxes. This was explicitly shown in the main text. Here we recap what are the correlations that win the magic square game and comment some characteristics of them.

First, the original definition of the game relies on the conditions to fill a table of 3×3 . These conditions can always be fulfilled using the observables in the Peres-Mermin magic

square

$\sigma_z \otimes \mathbb{1}$	$\mathbb{1} \otimes \sigma_z$	$\sigma_z \otimes \sigma_z$
$\mathbb{1} \otimes \sigma_x$	$\sigma_x \otimes \mathbb{1}$	$\sigma_x \otimes \sigma_x$
$\sigma_z \otimes \sigma_x$	$\sigma_x \otimes \sigma_z$	$\sigma_y \otimes \sigma_y$

At first glance this is a game with three inputs and eight outcomes. However, the third outcome for each measurement is completely determined from the conditions of the game. Therefore this can be recast as a three-input four-outcome game, (3,3,4,4) scenario. The specific measurements can be obtained by simultaneously diagonalizing the three operators in each row and column of Eq. (C1). The diagonalization yields 24 projectors, these can be arranged in six basis, which are distributed to Alice and Bob in the following way:

$$A^{0|0} = (1, 0, 0, 0), \quad B^{0|0} = (1, 1, 0, 0), \quad (\text{C2a})$$

$$A^{1|0} = (0, 1, 0, 0), \quad B^{1|0} = (1, -1, 0, 0), \quad (\text{C2b})$$

$$A^{2|0} = (0, 0, 1, 0), \quad B^{2|0} = (0, 0, 1, 1), \quad (\text{C2c})$$

$$A^{3|0} = (0, 0, 0, 1), \quad B^{3|0} = (0, 0, 1, -1), \quad (\text{C2d})$$

$$A^{0|1} = (1, 1, 1, 1), \quad B^{0|1} = (1, 0, 1, 0), \quad (\text{C2e})$$

$$A^{1|1} = (1, 1, -1, -1), \quad B^{1|1} = (1, 0, -1, 0), \quad (\text{C2f})$$

$$A^{2|1} = (1, -1, 1, -1), \quad B^{2|1} = (0, 1, 0, 1), \quad (\text{C2g})$$

$$A^{3|1} = (1, -1, -1, 1), \quad B^{3|1} = (0, 1, 0, -1), \quad (\text{C2h})$$

$$A^{0|2} = (1, 1, 1, -1), \quad B^{0|2} = (1, 0, 0, -1), \quad (\text{C2i})$$

$$A^{1|2} = (1, 1, -1, 1), \quad B^{1|2} = (1, 0, 0, 1), \quad (\text{C2j})$$

$$A^{2|2} = (1, -1, 1, 1), \quad B^{2|2} = (0, 1, -1, 0), \quad (\text{C2k})$$

$$A^{3|2} = (-1, 1, 1, 1), \quad B^{3|2} = (0, 1, 1, 0). \quad (\text{C21})$$

se projectors, together with the maximally entangled state

$= \frac{1}{2} \sum_i |ii\rangle$, produce the magic square correlations [19]:

These projectors, together with the maximally entangled state $|\psi\rangle = \frac{1}{2} \sum_i |ii\rangle$, produce the magic square correlations [19]:

$$\vec{p}_{MS} = \frac{1}{8} \times \left(\begin{array}{cc|cc|cc} 1 & 1 & 1 & 1 & 1 & 1 \\ 1 & 1 & & & 1 & 1 \\ & & 1 & 1 & 1 & 1 \\ & & 1 & 1 & & 1 \\ \hline 1 & 1 & 1 & 1 & & 1 \\ 1 & 1 & & 1 & 1 & 1 \\ 1 & 1 & 1 & 1 & 1 & 1 \\ \hline 1 & 1 & 1 & 1 & 1 & 1 \\ 1 & 1 & & 1 & 1 & 1 \\ 1 & 1 & 1 & 1 & 1 & 1 \\ \hline 1 & 1 & 1 & 1 & 1 & 1 \end{array} \right) . \quad (C3)$$

Using the magic square correlations \vec{p}_{MS} is straightforward to find a Bell inequality that is violated up to the algebraic maximum of 9 by them

$$B_{MS} = \left(\begin{array}{cc|cc|cc} 1 & 1 & 1 & 1 & 1 & 1 \\ 1 & 1 & & 1 & 1 & 1 \\ & 1 & 1 & 1 & 1 & 1 \\ & 1 & 1 & & 1 & 1 \\ \hline 1 & 1 & 1 & 1 & 1 & 1 \\ 1 & 1 & & 1 & 1 & 1 \\ 1 & 1 & 1 & 1 & 1 & 1 \\ 1 & 1 & 1 & 1 & 1 & 1 \\ \hline 1 & 1 & 1 & 1 & 1 & 1 \\ 1 & 1 & & 1 & 1 & 1 \\ 1 & 1 & 1 & 1 & 1 & 1 \\ 1 & 1 & & 1 & 1 & 1 \end{array} \right). \quad (C4)$$

The magic square game is obtained simply by normalizing this inequality using the factor $1/9$.

Appendix D: LO² violation analysis examples

For the extremal box given in (A2), each event occurs with probability $\frac{1}{3}$, therefore to test for the violation of any LO² inequality, each clique event would occur with probability $\frac{1}{9}$. Hence, the condition of violation for a clique of size l , becomes:

$$\frac{l}{9} > 1. \quad (D1)$$

Therefore, the violating clique will be of size 10 or more. Our code found a K_{10} that violates the corresponding LO² inequality. The set of those 10 locally orthogonal events being: $\{2021|0002, 2001|0002, 1020|1112, 1120|0120, 1111|0010, 1101|0010, 2000|1022, 0101|0010, 0120|0120, 0111|0010\}$.

We now move to the extremal boxes of scenario (2,3,3,3) and start with the box given in Eq. (A3). Running our code for this box, we obtain a K_{12} that violates the corresponding LO² inequality. The set of these 12 locally orthogonal events being: $\{0212|0110, 0201|1012, 1002|1211, 1111|0001, 2012|0110, 1120|0202, 1102|0202, 2202|1211, 2222|1211, 2220|1211, 2020|0210, 2021|0210\}$.

For the extremal box in Eq. (A4), we also get a K_{12} that violates the corresponding LO² inequality. The set of these 12 locally orthogonal events being: $\{0212|0111, 0211|0001, 0120|1211, 2022|1012, 1020|1211, 2111|0010, 2001|0211, 2101|0211, 1221|0202, 1220|0202, 1102|0001, 1111|0001\}$.

For the extremal box in Eq. (A5), a clique of size 10 or more will be needed. We found a K_{10} , and the corresponding set of 10 mutually orthogonal events are: $\{0211|1101, 0220|1101, 1102|0200, 0202|0200, 2002|0110, 2020|1010, 2011|1010, 1022|1212, 1111|1102, 1120|1102\}$.

Appendix E: Communication complexity

For scenarios in which we can obtain complete lists of classes of extremal NS points, we can test how much communication is required to reproduce the correlations of these different points. In [Table II](#), we give the results of our extensive computations, based on which we obtain violations of LHV+dit for $d \leq 5$, the highest communication complexity being achieved in the scenario $(6, 4, 2, 2)$.

Now we prove the assertion in the main text concerning the arbitrary communication complexity of NS strategies. In the scenario $(m, m, 2, 2)$, recall that

$$p = \begin{pmatrix} C & C & \cdots & C \\ \hline C & A & \cdots & C \\ \hline \vdots & \vdots & \ddots & \vdots \\ \hline C & C & \cdots & A \end{pmatrix}, \quad (\text{E1})$$

where

$$C = \begin{pmatrix} \frac{1}{2} & 0 \\ 0 & \frac{1}{2} \end{pmatrix} \quad \text{and} \quad A = \begin{pmatrix} 0 & \frac{1}{2} \\ \frac{1}{2} & 0 \end{pmatrix}, \quad (\text{E2})$$

and define $F = 4p - 1$. In other words, F has entries

$$F(ab|xy) = \begin{cases} 1 & \text{if } a + b = (1 - \delta_{x,1})\delta_{x,y} \pmod{2}, \\ -1 & \text{otherwise.} \end{cases} \quad (\text{E3})$$

Consider $d \leq m$, we want to obtain the value of the bound LHV+dit for the inequality F . Without loss of generality, we can restrict to the case where Alice's deterministic strategy is to always return her first output.

If $d = m$, then it is trivial that the NS value m^2 can be achieved, as Alice can simply communicate her input to Bob, who has then perfect information to obtain score one for the inequality F for all values of x and y .

If $d < m$, then, by symmetry of F , the choice of the communication function is only relevant with respect to the first input, and it is easy to see that one optimal strategy is to communicate 1 for $x \in [1, m-d+1]$ and $x-d$ for $x \in [m-d+2, m]$. When Bob receives 1, he is indeed left with a reduced version of the inequality F (of size $m-d+1$), for which his optimal strategy is to always return his first output, only losing when $x = y \in [2, m-d+1]$; otherwise, he has perfect knowledge. Combining both paths, we obtain the announced value of $m^2 - 2(m-d)$.

A = 2 and B = 2

X	Y	#L1	#L2	#L3	#L4	#L5
2	2	1	$\frac{1}{2}$.	.	.
2	3	2	$\frac{1}{2}$.	.	.
2	4	4	$\frac{1}{2}$.	.	.
2	5	6	$\frac{1}{2}$.	.	.
2	6	9	$\frac{1}{2}$.	.	.
2	7	12	$\frac{1}{2}$.	.	.
2	8	16	$\frac{1}{2}$.	.	.
2	9	20	$\frac{1}{2}$.	.	.
3	3	4	$\frac{1}{2}$	1	$\frac{11}{15}$.
3	4	11	$\frac{1}{2}$	3	$\frac{2}{3}$.
3	5	18	$\frac{1}{2}$	6	$\frac{2}{3}$.
3	6	29	$\frac{1}{2}$	11	$\frac{2}{3}$.
3	7	42	$\frac{1}{2}$	18	$\frac{2}{3}$.
3	8	60*	$\frac{1}{2}$	28	$\frac{2}{3}$.
4	3	11	$\frac{1}{2}$	3	$\frac{2}{3}$	1
4	4	19	$\frac{5}{12}$	9	$\frac{15}{8}$	5
4	5	52	$\frac{2}{5}$	28	$\frac{15}{8}$	13
4	6	97*	$\frac{2}{5}$	61	$\frac{5}{8}$	32
5	3	18	$\frac{1}{2}$	6	$\frac{2}{3}$	2
5	4	52	$\frac{2}{5}$	28	$\frac{5}{8}$	13
5	5	72	$\frac{15}{38}$	51	$\frac{31}{55}$	31
6	3	29	$\frac{1}{2}$	11	$\frac{2}{3}$	4
6	4	97*	$\frac{2}{5}$	61	$\frac{5}{8}$	34
7	3	42	$\frac{1}{2}$	18	$\frac{2}{3}$	7
8	3	60*	$\frac{1}{2}$	28	$\frac{2}{3}$	12

(a)

A = 2 and B = 3

X	Y	#L1	#L2	#L3
2	2	1	$\frac{1}{2}$.
2	3	2	$\frac{1}{2}$.
2	4	4	$\frac{1}{2}$.
2	5	6	$\frac{1}{2}$.
2	6	9	$\frac{1}{2}$.
2	7	13	$\frac{1}{2}$.
3	2	3	$\frac{1}{2}$.
3	3	16	$\frac{5}{11}$	3
3	4	89	$\frac{7}{16}$	26
4	2	13	$\frac{1}{2}$	4
4	3	427	$\frac{5}{11}$	316
5	2	56	$\frac{1}{2}$	35

(c)

A = 3 and B = 2

X	Y	#L1	#L2	#L3
2	2	1	$\frac{1}{2}$.
2	3	3	$\frac{1}{2}$.
2	4	13	$\frac{1}{2}$.
2	5	56	$\frac{1}{2}$.
3	2	2	$\frac{1}{2}$.
3	3	16	$\frac{5}{11}$	5
3	4	427	$\frac{5}{11}$	343
4	2	4	$\frac{1}{2}$.
4	3	89	$\frac{7}{16}$	51
5	2	6	$\frac{1}{2}$	1
6	2	9	$\frac{1}{2}$	$\frac{13}{16}$
7	2	13	$\frac{1}{2}$.

(e)

A = 2 and B = 4

X	Y	#L1	#L2	C_{\max}
2	2	1	$\frac{1}{2}$	5
2	3	2	$\frac{1}{2}$	5
2	4	4	$\frac{1}{2}$	5
2	5	6	$\frac{1}{2}$	5
3	2	3	$\frac{15}{31}$	7
3	3	18	$\frac{3}{7}$	10
4	2	16	$\frac{15}{31}$	11
5	2	202*	$\frac{15}{31}$	15

(d)

A = 4 and B = 2

X	Y	#L1	#L2	C_{\max}
2	2	1	$\frac{1}{2}$	5
2	3	3	$\frac{15}{31}$	7
2	4	16	$\frac{15}{31}$	11
2	5	202*	$\frac{15}{31}$	15
3	2	2	$\frac{1}{2}$	5
3	3	18	$\frac{3}{7}$	10
4	2	4	$\frac{1}{2}$	5
5	2	6	$\frac{1}{2}$	5

(f)

A = 3 and B = 3

X	Y	#L1	#L2	C_{\max}
2	2	2	$\frac{8}{17}$	10
2	3	22	$\frac{8}{17}$	12
2	4	379	$\frac{8}{17}$	16
3	2	22	$\frac{8}{17}$	12
3	3	8747*	$\frac{13}{31}$	20
4	2	379	$\frac{8}{17}$	16

(b)

Remaining scenarios

X	Y	A	B	#L1	#L2	C_{\max}
2	2	3	4	2	$\frac{5}{11}$	10
2	2	4	4	3	$\frac{3}{7}$	17
2	2	5	5	4	$\frac{16}{41}$	26
2	3	3	4	28	$\frac{5}{11}$	14
2	3	4	3	104	$\frac{5}{11}$	19
3	2	3	4	104	$\frac{5}{11}$	19
3	2	4	3	28	$\frac{5}{11}$	14
3	2	4	3	18	$\frac{11}{15}$	14

(g)

TABLE II. Number of classes of ENS boxes which violate different communication scenarios. For each scenario given, we have a list of classes that is complete, which we could prove in most of them, and only conjecture for some which we indicate with a star. Next to the number of boxes that cannot be reproduced with communication d , we indicate the minimum visibility with respect to the corresponding polytope, that is, the ratio of the LHV+dit value to the NS one. We provide C_{\max} , the largest clique size we found in the scenario. For $A \cdot B \leq 6$, we have $C_{\max} = 5$. For concision, we only provide results for one version of each set of two party-symmetric scenarios.